Available online at www.sciencedirect.com

ScienceDirect

IFAC PapersOnline CONFERENCE PAPER ARCHIVE

IFAC PapersOnLine 55-9 (2022) 48–53

Phase current estimation based shunt active power compensation

Márton Greber * **Attila Fodor** * **Attila Magyar** *

* *Department of Electrical Engineering and Information Systems, Faculty of Information Technology, University of Pannonia, Egyetem u. 10., Veszprém, H-8200, Hungary(e-mail: greber.marton, fodor.attila, magyar.attila@virt.uni-pannon.hu).*

Abstract: Nonlinear and unbalanced loads introduce distortions to the power network in the form of harmonics and asymmetric load conditions. Through the rising penetration of residential renewable plants, energy is fed back into the grid. By shaping the output of those power converters the distortions can be mitigated. The technique of shunt active power filtering allows the instantaneous compensation of a dedicated nonlinear load, by measuring its distorted consumption. The goal of this article is to present an extension to this method which allows to compensate for a given area utilizing the advanced metering infrastructure in a smart grid. Given a compensation unit, instantaneous voltage measurements are collected from neighboring consumers. By utilizing the model of the distribution line, a linear Kalman filter allows the estimation of the phase currents. These values replace the dedicated nonlinear load measurements, and by compensating for line currents, the power quality of a given transformer area is improved. Analyzing the model based approach against real world like scenarios and elaborating the robustness shows the potential for real world applicability.

Copyright © 2022 The Authors. This is an open access article under the CC BY-NC-ND license (https://creativecommons.org/licenses/by-nc-nd/4.0/)

Keywords: Smart grids; Optimal operation and control of power systems; Control of renewable energy resources; Instantaneous power theory; Active power filtering

1. INTRODUCTION

The electrical distribution system is responsible for the delivery of electrical power to the end customers. The demand posed by symmetrical linear loads is supplied by the utility as balanced three phase, sinusoidal quantities. However nonlinear loads introduce harmonic distortion to the lines by drawing currents with higher harmonic content regarding the base frequency. The power network is designed to operate under sinusoidal conditions, however distortions may force it outside of this nominal state. (Kordestani et al. (2017)) Harmonic distortion can result in the overheating of transformers and electric machines. If the power factor of a given load is not unity, reactive power is drawn from the grid, which accomplishes no effective work, but contributes to the current flow in the distribution line. In case of balanced system operation there is no zero sequence current present in the network. Another undesirable effect is unbalance with respect to phase quantities. Unbalance can originate from asymmetrical three phase loads, or unevenness with regards to spatial distribution of single phase customers. This results in the appearance of zero sequence currents, which introduce additional losses to the system. If one considers some of the general characteristics of residential distribution grids:

- power supplies: diode bridge with input capacitance,
- single phase induction motors: power factor ~ 0.9,
- spatial distribution of residential households on the phases,

it can be observed that harmonic distortion, reactive power flow and asymmetry can be all observed in the network. The world average transmission and distribution (T&D) loss value is around 8%, data broken down into regions is shown in table 1. (The World Bank (2014)) It can be observed that by reducing the aforementioned distortions, a part from the T&D losses could be reduced which is greatly beneficial.

Table 1. Electric power transmission and distribution losses(The World Bank (2014))

Region	Losses
North America	6%
Europe & Central Asia	8%
Middle East & North Africa	13%
Arab world	14%
Latin America & Caribbean	16%

Existing methods of power quality enhancement, and loss reduction can be categorized as either passive or active. By installing capacitor banks for reactive power compensation, or harmonic filters out of LC components, passive solutions are obtained. (Das (2015)) The notion of flexible AC transmission system involves the utilization of semiconductor switches for series and/or shunt compensation. (Watanabe et al. (2018)) Both of these solutions are designed to account for a dedicated source of distortion. For example an industrial site with low power factor would install its own capacitor banks for reactive power compensation. The effect of a nonlinear load with significant power requirement is mitigated by installing a dedicated shunt active filter to cancel out harmonics as close as possible.

2405-8963 Copyright © 2022 The Authors. This is an open access article under the CC BY-NC-ND license.
Peer review under responsibility of International Federation of Automatic Control.
10.1016/j.ifacol.2022.07.009

Through distributed generation (DG) energy sources get closer to the consumer points thereby the T&D losses are smaller. Aside from feeding sinusoidal AC power into the grid, the output waveform can be modulated to increase power quality of a transformer area. (Garcia-Torres et al. (2020)) Shunt compensators measure the load current of a dedicated nonlinear device and compensate for that. However to accomplish DG based compensation of an area, the line currents are required. However considering residential DG points, it is not feasible to measure the distribution line currents. This poses the bottleneck of the problem. By using the voltage at the point of common coupling (PCC), the line disturbances can be estimated through optimization. Applying this method for photovoltaic (PV) inverters a controller has been presented which reduced total harmonic distortion (THD) down to 5.04%. (Görbe et al. (2012)) Another method involved the utilization of PCC voltage measurements and PV inverters to calculate the voltage unbalance, and using this metric compensate for the asymmetry thereby increasing power quality. (Neukirchner et al. (2017))

These methods proved that compensation for a transformer area is possible without line current data, only using PCC measurements. Separate controllers has been presented for different aspects of power quality. *The aim of this work is to present a method to increase power quality in all three aspects - harmonics, reactive power and unbalance - by utilizing DG power converters and relying only on voltage measurement data.*

2. ACTIVE POWER FILTERING

The foundation of the proposed method is the classical shunt active power filter (SAPF) methodology. The principle of the filter is depicted in figure 1. There is an arbitrary nonlinear load consuming i_L current, the goal of the power converter is to provide the compensation current i_C in such a way that the utility must only supply sinusoidal, balanced i_S. If one requires such i_S and the load i_L is given, Kirchhoff's current law results in the instantaneous compensation current:

$$i_C = i_L - i_S. \tag{1}$$

The SAPF consists of a semiconductor bridge, an intermediate capacitor and some coupling inductances. The dedicated compensation is accomplished in such a way, that the controller uses the load current and PCC voltage as inputs. Only the switching losses are consumed from the network, the SAPF is self sustaining, a capacitor bank is only needed for intermediate energy storage. The controller utilizes the instantaneous power theory or also called p-q theory, developed by Hirofumi Akagi. A brief overview is given about the method, detailed discussion is omitted, since it is just a tool in the context of this article. Detailed explanation can be found in the original publication. (Akagi et al. (2017)) The method is based on the $\alpha\beta$ transformation. This converts the instantaneous values of the *abc* phases into the $\alpha\beta$ axes.

Using the $\alpha\beta$ voltages and currents, the power can be calculated as voltage times the current conjugate. Reformulating this statement, the instantaneous powers p and q can ba calculated:

$$\begin{bmatrix} p \\ q \end{bmatrix} = \begin{bmatrix} u_\alpha & u_\beta \\ u_\beta & -u_\alpha \end{bmatrix} \begin{bmatrix} i_\alpha \\ i_\beta \end{bmatrix}. \tag{2}$$

This power definitions are valid for both steady-state and transient, nevertheless also for arbitrary waveform shapes. p is the instantaneous real power, q is the instantaneous imaginary power Both p and q can be separated into average and oscillating parts:

$$\begin{aligned} p &= \overline{p} + \tilde{p}, \\ q &= \overline{q} + \tilde{q}, \end{aligned} \tag{3}$$

where $\overline{p}$, $\overline{q}$ are the average values, $\tilde{p}$, $\tilde{q}$ are the oscillating quantities. The average values of the p-q theory represent the same quantities as the classical three phase active and reactive power definitions. $\tilde{p}$ represents oscillating power flow thereby it results in zero average value and no power is transferred. $\tilde{q}$ accounts for power transferred between the phases, it represents no power transported from source to the load. It can be observed that $\tilde{p}$, $\overline{q}$ and $\tilde{q}$ are unwanted components, by decreasing these, the efficiency and thereby power quality of the system can be improved.

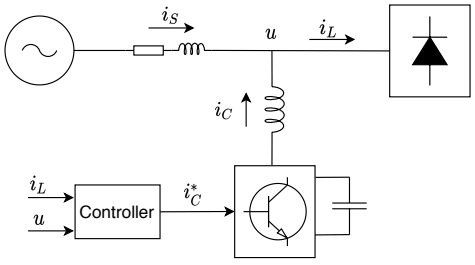

Fig. 1. Shunt active power filter: the nonlinear load's distorted consumption is compensated by a self sustained active device

The p-q control algorithm starts by taking the measured currents and voltages at the point of common coupling (u and i_L in figure 1.) and converting them to the $\alpha\beta$ reference frame. The instantaneous power values are calculated using equation 2. The average power is separated through a low-pass filter, such that the oscillating part is obtained, which we want to decrease. In order to keep the DC voltage of the capacitor controlled, the inverter's switching losses ($\overline{p}_{loss}$) are covered by adding it to the active power. The reactive power is not manipulated since we want to decrease both parts - average and oscillating as well - of it. The desired power signals to achieve power quality improvement are: $-\tilde{p} + \overline{p}_{loss}$ and $-q$. To get the appropriate control signals (i_C^*) for the inverter bridge, the current values from the instantaneous powers are calculated. Finally the $\alpha\beta$ quantities are transformed back to the *abc* domain.

3. PHASE CURRENT BASED COMPENSATION

The aim of this work is to present a method, such that power quality improvement can be accomplished not just for a dedicated load, rather a given transformer area. The classical SAPF approach is not enough since there is no single nonlinear load and thereby load current measurement, for which compensation can be done. Let us consider the configuration presented in figure 2. The transformer feeder point is represented as an ideal voltage source.

There are three, three phase consumers, the first is a regular P,Q type customer and the customer to the right is a nonlinear load. The household in the middle is equipped with DG capability, thereby contains a grid connected power converter. In order to simplify the derivations, this household's consumption is neglected, furthermore the DG system's renewable energy harvesting technology is also omitted in order to neglect the stochastic power input. The residential renewable system is considered as a SAPF. It is a three phase, three wire system in which the distribution lines consist of series RL branches. Mutual coupling between the phase conductors is neglected. Furthermore advanced metering infrastructure (AMI) is considered: the PQ and the nonlinear load are equipped with smart meters capable to measure instantaneous voltages and sending it to the SAPF. The communication is assumed to be ideal, there are no communication delays, bandwidth limitations nor packet losses.

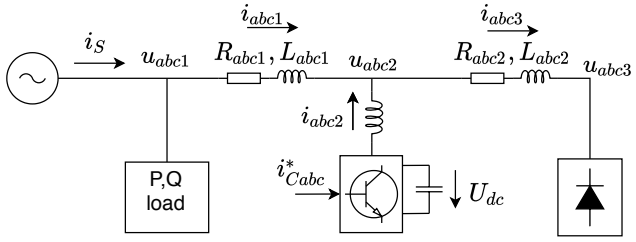

Fig. 2. Minimal line current estimation example

A single feeder radial layout is considered which is characteristic for low-voltage distribution networks. The power flow directions are considered to be known, for example in the presented case power flows from the distribution transformer as follows: PQ load, SAPF and finally the nonlinear load. The SAPF based on instantaneous power theory is taken as the power quality enhancement algorithm's foundation. In order to be able to compensate the nonlinear load from the customer with SAPF, the line current must be determined. Using it with the PCC voltage measurement, the network downstream of the SAPF can be compensated. From the SAPF's point of view this figuratively means, that the rest of network is considered as a Norton equivalent. In this case it can be clearly seen how it is similar to the classical SAPF approach.

3.1 The state-space model for estimation

The currents in the live distribution line conductors can't be measured, they need to be estimated. The power distribution line is a linear system, a linear Kalman filter can be applied to tackle the phase current estimation problem. In order to use this construct, an appropriate model is required. Let us first observe the single phase equivalent circuit of 2, which is depicted in figure 3. The voltages u_1 and u_3 represent the neighboring consumers with respect to the SAPF. i_1 and i_3 are the phase currents to be estimated. u_2 is the voltage at the PCC of the power converter and i_2 is the compensation current of the SAPF. By using kirchhoff's voltage and current laws, and the electrical equations of the components, the $\boldsymbol{A}$ and $\boldsymbol{B}$ matrices of continuous time state space model are obtained. The state variables are the line inductor currents.

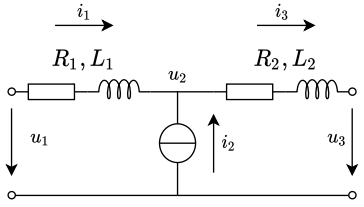

Fig. 3. Line model, single phase circuit

In order to provide measurement data for the Kalman filter, the output equation must be chosen in such a way, that it should represent a measurable quantity. By observing the PCC of the SAPF and formulating Kirchhoff's current law (KCL) it can be seen that i_2 can be expressed in terms of the state variables. The final form of the state-space model is shown in equation 4.

$$\begin{bmatrix} \frac{di_1}{dt} \\ \frac{di_3}{dt} \end{bmatrix} = \begin{bmatrix} -\frac{R_1}{L_1} & 0 \\ 0 & -\frac{R_2}{L_2} \end{bmatrix} \begin{bmatrix} i_1 \\ i_3 \end{bmatrix} + \begin{bmatrix} \frac{1}{L_1} & -\frac{1}{L_1} & 0 \\ 0 & \frac{1}{L_2} & -\frac{1}{L_2} \end{bmatrix} \begin{bmatrix} u_1 \\ u_2 \\ u_3 \end{bmatrix}$$
$$y = [-1 \ 1] \begin{bmatrix} i_1 \\ i_3 \end{bmatrix} \tag{4}$$

The $\boldsymbol{C}$ matrix is just the formulation of KCL, such that later the measured compensation current can be used as the measured output quantity. However this model needs to be extended to a three phase model, such that power filtering can be performed. The notations explained here are also used in figure 2. Single phase current and voltage quantities are collected into vectors, for example all the phase currents belonging to subscript 1 are put together into the vector $\boldsymbol{i_{abc1}}$:

$$\boldsymbol{i_{abc1}} = [i_{a1} \ i_{b1} \ i_{c1}]. \tag{5}$$

Distribution line parameters like phase resistance and inductance are organised into diagonal 3×3 matrices, for example the first three phase line section's resistance values are collected the following way:

$$\boldsymbol{R_{abc1}} = diag([R_{a1} \ R_{b1} \ R_{c1}]). \tag{6}$$

Using these definitions the state-space model in equation 4. is extended to phases *abc*. The state vector consists of the two, three phase line currents, the input vector is formed from the three, three phase voltages:

$$\begin{aligned} \boldsymbol{x} &= [\boldsymbol{i_{abc1}} \ \boldsymbol{i_{abc3}}]^T, \\ \boldsymbol{u} &= [\boldsymbol{u_{abc1}} \ \boldsymbol{u_{abc2}} \ \boldsymbol{u_{abc3}}]^T. \end{aligned} \tag{7}$$

Following the same steps which were described in the single phase case, the model can be formulated in the *abc* three phase reference frame:

$$\begin{aligned} \boldsymbol{A} &= \begin{bmatrix} -\boldsymbol{R_{abc1}}(\boldsymbol{L_{abc1}}^{-1}) & \boldsymbol{0}_{3\times3} \\ \boldsymbol{0}_{3\times3} & -\boldsymbol{R_{abc2}}(\boldsymbol{L_{abc2}}^{-1}) \end{bmatrix}, \\ \boldsymbol{B} &= \begin{bmatrix} \boldsymbol{L_{abc1}}^{-1} & -\boldsymbol{L_{abc1}}^{-1} & \boldsymbol{0}_{3\times3} \\ \boldsymbol{0}_{3\times3} & \boldsymbol{L_{abc2}}^{-1} & -\boldsymbol{L_{abc2}}^{-1} \end{bmatrix}, \\ \boldsymbol{C} &= [-\boldsymbol{I}_{3\times3} \ \boldsymbol{I}_{3\times3}]. \end{aligned} \tag{8}$$

The linear discrete time (DT) Kalman filter to be used is described in equation 9. The matrices described in equa-

tion 8. must be converted using an appropriate sampling time, from continuous to discrete time.

$$\begin{aligned} \boldsymbol{x}[k+1] &= \boldsymbol{A}_d\boldsymbol{x}[k] + \boldsymbol{B}_d(\boldsymbol{u}[k] + \boldsymbol{w}[k]) \\ \boldsymbol{y}[k] &= \boldsymbol{C}_d\boldsymbol{x}[k] + \boldsymbol{v}[k] \end{aligned} \tag{9}$$

The model contains two noise terms: $\boldsymbol{w}[k]$ as the process noise and $\boldsymbol{v}[k]$ for the observation noise. Both of these are assumed to be zero mean Gaussian white noises with diagonal covariance matrices $\boldsymbol{Q}$ and $\boldsymbol{R}$:

$$\begin{aligned} \boldsymbol{w}[k] &\sim \mathcal{N}(0, \boldsymbol{Q}), \\ \boldsymbol{v}[k] &\sim \mathcal{N}(0, \boldsymbol{R}). \end{aligned} \tag{10}$$

$\boldsymbol{w}[k]$ acts on the inputs of the model. This noise originates from the voltage measurement errors from the neighboring consumers regarding the SAPF. $q_{1,1} \dots q_{3,3}$ and $q_{7,7} \dots q_{9,9}$ are the variances of the smart metering devices, whereas $q_{4,4} \dots q_{6,6}$ are the voltage measurement variances of the SAPF. The output of the state-space model is the SAPF current, the measurement variance is encapsulated in the diagonal elements of the matrix $\boldsymbol{R}$.

3.2 Phase current estimation based control

Integrating the previously elaborated distribution line model and the Kalman filter allows the estimation of the line currents. This can be used to extend the SAPF control algorithm for a more flexible operation mode. The proposed control scheme is depicted in figure 4. Voltage measurement data is received from the neighboring loads, furthermore the PCC of the SAPF is measured, these form the vector $\boldsymbol{u}$. Smart meters can have measurement errors, they are incorporated as additive noise. The observation for the Kalman filter is the SAPF current injection, denoted by $\boldsymbol{y}$. This can have also measurement error. These parameters are fed into the Kalman filter, such that the output is the optimal estimate of the line currents. In order to acquire the signal to be compensated for, KCL must be applied at the PCC. The estimated line current and the output current provide the distorted current. This was denoted by i_L in the classical SAPF approach, which must be compensated.

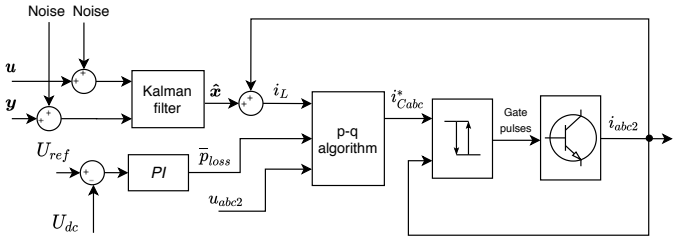

Fig. 4. Phase current estimation SAPF control strategy

From this point on, the same p-q control method can be applied which was explained at the beginning. The $\overline{p}_{loss}$ is shown explicitly, to make the loss power of the SAPF visible in the block diagram. The measured voltage at the PCC is fed also into the p-q block thereby giving all the necessary input quantities for power filtering. The ideal compensation waveform is generated which is denoted by i^*_{Cabc}. The actuator for the method is an inverter bridge, which is driven by a hysteresis controller. i^*_{Cabc} is fed into the hysteresis block, together with a feedback loop containing the output current.

Since in the modeling section the minimal conditions are assured for comprehensive description, some remarks about the relaxation of those are mentioned here. The control algorithm in this form doesn't account for voltage unbalance, only for current unbalance. This is an already solved problem, it was just omitted for sake of simplicity. It can be solved by filtering the PCC voltage components through a positive sequence voltage detector. (Akagi et al. (2017)) In case the renewable source is active, real power needs to be fed into the network through the SAPF. One way of accomplishing this is to subtract the generated power from the $\overline{p}_{loss}$. This is then fed into the p-q block which will then calculate the waveform, taking into consideration the generated power.

4. ANALYSIS

Based on the complex nature of the distribution system, that is equipped with power filtering device, the proposed algorithm is evaluated based on simulation results. The system depicted in 2. is implemented in Simulink. The feeder is a voltage generator supplying 400 V phase to phase. The parameters for both of the RL distribution line segments are 10 mΩ and 1 μH. The intermediate voltage of the SAPF is supplied by two 400 μF capacitors. The measurement error of the smart meters regarding the neighboring loads to the SAPF is 5%, for the SAPF it is under 1%. In order to simplify the scenario, the PQ load, left to the SAPF is set to have no power consumption. It only serves as a measurement data provider. The nonlinear load is a resistive load behind a capacitive rectifier stage. To account for further harmonic content, this unit is extended with additional current source having harmonic content.

One important aspect of such smart metering based applications is the evaluation of robustness against measurement errors. Experiments were conducted in which this disturbance was increased with regards to the neighboring nodes, that provide voltage data. The SAPF sensors are of higher precision, since the converter's inner control loops are dependent on those. (Aourir et al. (2020)) Thereby it is safe to assume that these measurements are not subject to change. The performance of the SPAF is defined as the reduction of the harmonic distortion, zero sequence currents and reactive power. By increasing the neighboring meter's voltage measurement error, no significant performance degradation was observed. This follows from that fact, that the Kalman filter provides optimal estimate, with a covariance less than the process and measurement noise. Since the measurement noise is of higher quality, the method is robust with respect to this kind of errors. The region of robust stability is evaluated by considering the reactive power consumption represented by the input stage capacitance (C_{load}), and the harmonic content of the load current (THD_{load}). Robust stability is considered as the ability to hold the performance metrics: THD under 5%, reduction of the reactive power by 85% and reduction of zero sequence currents by 90%. The parametric bounds of the robust stability are covered from experimental results:

$$\begin{aligned} \mathcal{D}_{THD_{load},C_{load}} = \{(THD_{load}, C_{load})| \\ 0\% < THD_{load} < 40\%, 1\ \mu\text{F} < C_{load} < 10\ \text{mF}\}. \end{aligned} \tag{11}$$

Increasing the parameters further resulted in the off-nominal operation -with regards to voltage levels, and

harmonic dominance- of the grid. The nominal working states on the other hand are covered by this bounds.

4.1 Robustnes agains time varying load

The instantaneous consumption of the loads in the grid can change over time. Therefore the effect of time varying nonlinear load is investigated. A similarly parameterized test case is created as elaborated before. There is some initial load on the network and the SAPF is turned on at $t = 10$ ms. The controller starts to compensate the grid, however at $t = 20$ ms the unbalanced load is increased both in harmonic content, active and reactive power. Robustness against time varying asymmetry is depicted on figure 5. The controller starts to compensate for the initial unbalance. However when the unbalance is increased instantaneously, the controller holds the compensated zero sequence source current levels.

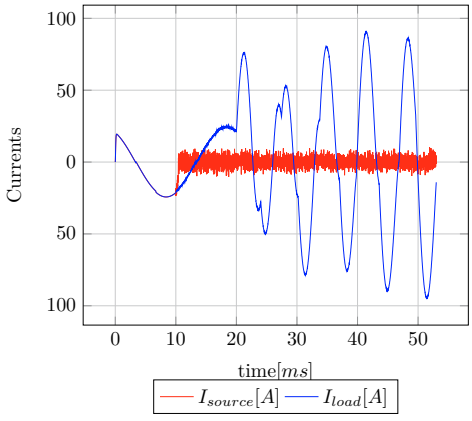

Fig. 5. Zero sequence currents: time varying unbalance

In case of the power curves, the controller compensates for the oscillating active power components, as well as the oscillating and average reactive power components, see figure 6. Between $10-20$ ms there is already no oscillating part in the active and reactive power of the source. No matter the increase in reactive power consumption at $t = 20$ ms the compensated reactive power level at the source is maintained.

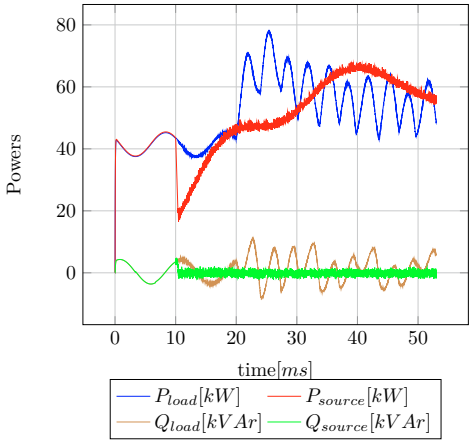

Fig. 6. Active and reactive powers: time varying average and oscillating power consumption

The THD calculation requires a whole period of the fundamental frequency, to produce results. This is the reason why figure 7. has a 20 ms lag. Therefore the increase in harmonic content starts at $t = 40$ ms on the plot. Nonetheless this does not effect the controller's performance metric. The source current harmonic content reaches a level below 5%.

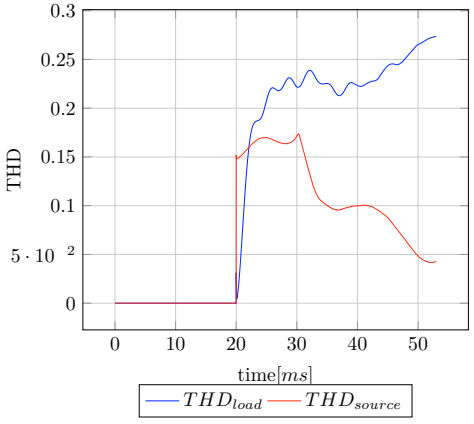

Fig. 7. Total harmonic distortions: time varying harmonic content presence

4.2 Robustnes against realistic pole configuration

A quite unlikely but possible source of error can originate from wrong cable parameters (length, spacing). Furthermore distribution lines can have mutual couplings. Because of the nature of model based methods, the effect of these phenomena are examined. A realistic line model based on geometries and conductor material data is implemented from fundamental distribution system literature. (Kersting (2012), page 92, figure 8.) The realistic distribution line model equations are worked out using the modified Carson's equations ("conductors and images"), using the Kron reduction technique the neutral wire is accounted for. The phase conductors are of type: "336,400 26/7 ACSR", the neutral wire is "4/0 6/1 ACSR". The R,L and C matrices are calculated using these data. The capacitive and inductive couplings in a realistic line model are validated through the non-zero off diagonal elements.

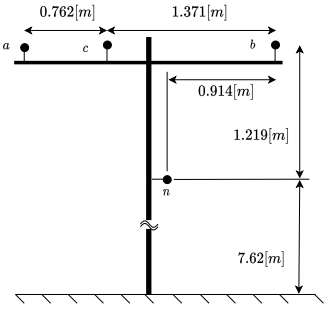

Fig. 8. Realistic pole configuration, used for simulations

A simulation test case was created incorporating the elaborated line model. The distance between the loads and the SAPF was chosen to be 100 m. Using measurements from the realistic model, the experimental results provided no significant performance degradation. In order to observe the performance of the compensator under such effects,

which are not accounted for in the model, detailed simulations were carried out. As the line segment gets longer, the effect of mutual coupling becomes not negligible. If the pole configuration contains uncertain data regarding the spacing of the conductors, errors will be introduced. The method is tested by increasing the length of the line segment (l). Furthermore the spacing of the conductors (Δs) is increased gradually. The results regarding the change in THD are shown in figure 9, reactive power and zero sequence currents have shown a similar trend. The parametric bounds of robustness against these error factors, which originate from modeling assumptions are the following:

$$\mathcal{D}_{l,\Delta s} = \{(l, \Delta s)| \\ 0 \text{ m} < l < 200 \text{ m}, 0 \text{ m} < \Delta s < 0.5 \text{ m}\}. \quad (12)$$

The bounds of l mean that the effects of mutual coupling can be neglected as long as the distance between neighboring loads is less than 200 m. 0.5 m increase in the geometrical spacing of the conductors on the pole meets the engineering expectations. Bigger changes in the value of Δs would most likely indicate a damaged pole.

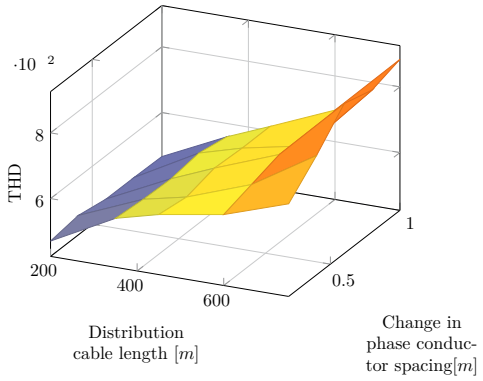

Fig. 9. Effect of realistic pole configuration on THD, perturbation of length and spacing. Effect on reactive power and zero sequence current results show a similar trend.

5. CONCLUSION

An extension to the classical shunt-active power filtering method based on p-q theory has been presented. It is a model based approach utilizing existing DG equipment and relies on voltage measurement data from neighboring consumers. The power filtering is accomplished on the estimated line currents, therefore power quality is improved not just for a given load, rather for a whole transformer area. The operating principle of the Kalman filter based SAPF is elaborated through a simulation example. The controller has been analyzed with respect to robustness against the distortion of the loads where parametric bounds were established. Furthermore response to time varying nonlinear loads has been examined. The method is tested against errors originating from modeling assumptions, like the utilization of a real pole configuration with mutual coupling. It has been shown that for relatively small distances < 200 m, the presented model is satisfactory. For networks with longer distance between loads(rural regions) the real pole configuration should be considered. Considering that the model uses existing equipment and requires only software/communication enhancements, the savings offer a good and easy to implement improvement for the future smart grids.

ACKNOWLEDGEMENTS

Project no. 131501 has been implemented with the support provided from the National Research, Development and Innovation Fund of Hungary, financed under the K_19 funding scheme. A. Magyar was supported by the János Bolyai Research Scholarship of the Hungarian Academy of Sciences. Attila Magyar was supported by the ÚNKP-21-5 New National Excellence Program of the Ministry for Innovation and Technology from the source of the National Research, Development and Innovation Fund.

REFERENCES

Akagi, H., Watanabe, E.H., and Aredes, M. (2017). *Instantaneous power theory and applications to power conditioning*. Wiley IEEE Press.

Aourir, M., Abouloifa, A., Aouadi, C., Otmani, F.E., Lachkar, I., Giri, F., and Guerrero, J.M. (2020). Nonlinear control of multicellular single stage grid connected photovoltaic systems with shunt active power filtering capability. *IFAC-PapersOnLine*, 53(2), 12853–12858. doi:https://doi.org/10.1016/j.ifacol.2020.12.2091. 21st IFAC World Congress.

Das, J.C. (2015). Passive filters. In *Power System Harmonics and Passive Filter Designs*, 685–743. John Wiley & Sons, Inc. doi:10.1002/9781118887059.ch15.

Garcia-Torres, F., Vazquez, S., Bordons, C., Moreno-Garcia, I., Gil, A., and Roncero-Sanchez, P. (2020). Power quality management of interconnected microgrids using model predictive control. *IFAC-PapersOnLine*, 53(2), 12918–12923. doi:https://doi.org/10.1016/j.ifacol.2020.12.2121. 21st IFAC World Congress.

Görbe, P., Magyar, A., and Hangos, K.M. (2012). Reduction of power losses with smart grids fueled with renewable sources and applying ev batteries. *Journal of Cleaner Production*, 34, 125–137. doi:10.1016/j.jclepro.2011.12.021.

Kersting, W. (2012). *Distribution System Modeling and Analysis, Third Edition*. Taylor & Francis.

Kordestani, M., Safavi, A.A., and Saif, M. (2017). Harmonic fault diagnosis in power quality system using harmonic wavelet. *IFAC-PapersOnLine*, 50(1), 13569–13574. doi:https://doi.org/10.1016/j.ifacol.2017.08.2370. 20th IFAC World Congress.

Neukirchner, L., Görbe, P., and Magyar, A. (2017). Voltage unbalance reduction in the domestic distribution area using asymmetric inverters. *Journal of Cleaner Production*, 142, 1710–1720. doi:10.1016/j.jclepro.2016.11.119.

The World Bank (2014). Electric power transmission and distribution losses. URL `https://data.worldbank.org/indicator/EG.ELC.LOSS.ZS`. Accessed: 2020.10.26.

Watanabe, E.H., deAraújo Lima, F.K., daSilva Dias, R.F., Aredes, M., Barbosa, P.G., Lima Barcelos, S.L., and Santos, G. (2018). 28 - flexible ac transmission systems. In M.H. Rashid (ed.), *Power Electronics Handbook (Fourth Edition)*, 885 – 909. Butterworth-Heinemann, fourth edition edition.